Polymer Journal, Vol. 18, No. 12, pp 973—980 (1986)

X-Ray Structural Study of Optically Active Polyamide, (+)-Poly((2*R*,6*S*)-tetrahydropyran-2,6-diyliminocarbonyl)

Zeyong ZHENG, Takashi YAMANE, Tamaichi ASHIDA, Kazuhiko HASHIMOTO,* and Hiroshi SUMITOMO*

*Department of Applied Chemistry, Faculty of Engineering, and *Faculty of Agriculture, Nagoya University, Chikusa, Nagoya 464, Japan*

(Received June 13, 1986)

ABSTRACT: The conformation of (+)-poly((2*R*,6*S*)-tetrahydropyran-2,6-diyliminocarbonyl) has been studied by the X-ray diffraction method. Crystal data: P2, $a=11.79$, $b=14.40$, c (fiber axis) $=19.43$ Å, $\gamma=98.0°$, $D_0=1.23\,g\,cm^{-3}$, $D_c=1.29\,g\,cm^{-3}$, $Z=20$. A double-stranded right-handed helix structure of a 10_3 symmetry is derived from the X-ray, IR dichroism and conformational analyses. The double-stranded helix is rather rigid because of the hydrogen bonds and several close contacts formed between the two single chains.

KEY WORDS Optically Active Polyamide / Bicyclic Oxalactam / Double Helix / 10_3 Helix / X-Ray Diffraction / IR Dichroism / Conformational Analysis /

An optically active polyamide, (+)-poly((2*R*,6*S*)-tetrahydropyran-2,6-diyliminocarbonyl) (abbreviated as (+)-poly(BOL)), is prepared from a bicyclic oxalactam, (+)-(1*R*,5*S*)-8-oxa-6-azabicyclo-(3.2.1)-octan-7-one [(+)-BOL], by the anionic solution polymerization through the N^6–C^7 scission of the amide group,[1] as well as a racemic polyamide (poly(BOL)).[2] (+)-Poly(BOL) and

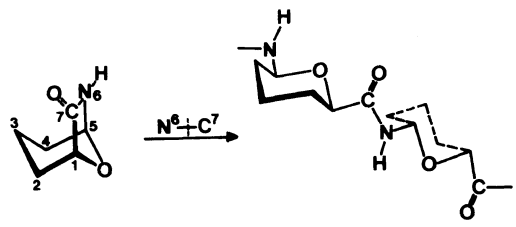

(+)-BOL (+)-poly(BOL)

Scheme

poly(BOL) are new functional polymers with water permeability and ion selectivity, consisting of an alternating arrangement of an amide moiety and a tetrahydropyran moiety.[1-3] The NMR spectra show that the carbonyl and the imino groups are equatorial with respect to the tetrahydropyran ring in the polyamides.[1,2] (+)-Poly(BOL) is more stable than poly(BOL) with respect to the physical and chemical properties. The melting and decomposition temperatures of (+)-poly(BOL) are 290—305°C and about 330°C, respectively,[1] and the glass transition point is about 160°C. Those of poly(BOL) are 260—285°C and about 315°C, and the glass transition point is 130°C.[1,2] For solubility, poly(BOL) is dissolved in trifluoroethanol (TFE), but (+)-poly(BOL) is not. The differences may be attributed to the structural regularity of (+)-poly(BOL), as compared with that of poly(BOL). Thus the X-ray structure analysis of the (+)-poly(BOL) film has been carried out to make the structure of (+)-poly(BOL) clear and obtain informations available for the molecular design of new functional polymers.

EXPERIMENTAL

Preparation of Specimen

The polymer was dissolved in a mixed solvent of TFE and $CHCl_3$ (the mixing ratio, *ca.* 1 : 3) at room temperature and cast into a film in a vacuum desiccator. Because of the brittleness of the film, it was swollen during stretching with $CHCl_3$. The largest stretching ratio reached so far is about 3.0 for the film with low crystallinity and 2.5 for that with relatively high one. The uniaxially oriented specimen was then annealed under tension in a vaccum at a temperature about 10°C above the glass transition point of the polymer for 24 h.

The observed density (D_0) of the film, 1.23 $g cm^{-3}$, was obtained with flotation in a hexane–tetrachloromethane solution.

IR Spectroscopy

An oriented film with the thickness of about 15 μm stretched by *ca.* 1.5 times was prepared and its IR dichroism was measured with a JASCO diffraction grating infrared spectrophotometer (IRA-2) using a wire grid polarizer. The resultant IR dichroism spectra of the oriented film of (+)-poly(BOL) are given in Figure 1.

X-Ray Diffraction Measurement

X-ray photographs of (+)-poly(BOL) were taken with an evacuated cylindrical camera with a diameter of 7.0 cm and a Weissenberg camera with a diameter of 5.73 cm using Ni-filtered Cu-K_α radiation. The camera radii

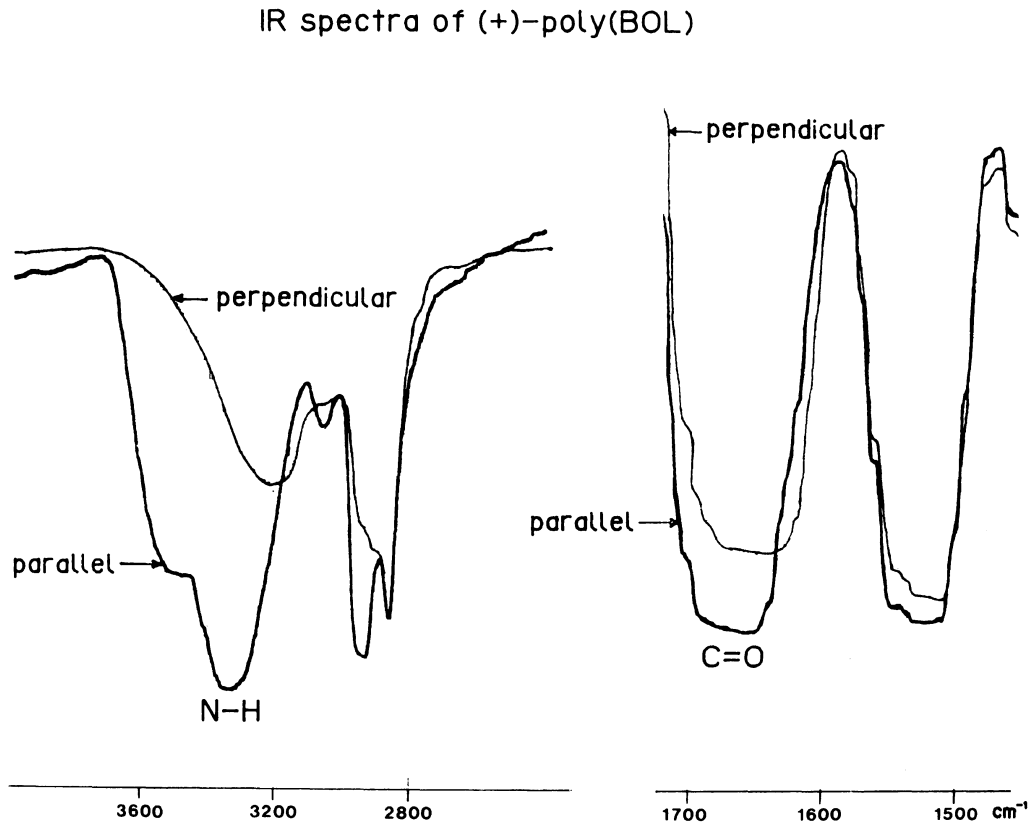

Figure 1. IR dichroism spectra of uniaxially oriented film of (+)-poly(BOL). Parallel, electric vector is parallel to the fiber axis; perpendicular, electric vector is perpendicular to the fiber axis.

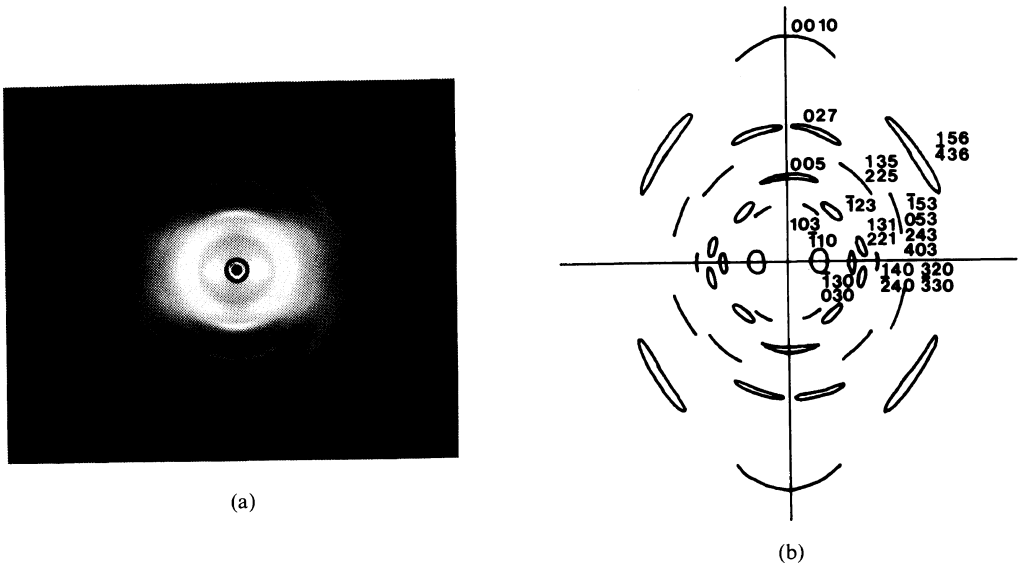

Figure 2. a) X-Ray fiber pattern of (+)-poly(BOL) (cylindrical camera, Cu-K_α radiation, fiber axis vertical); b) Schematic representation of the fiber pattern with their indices of the reflections.

were calibrated with the NaCl powder pattern. The intensities were measured with a microdensitometer, and Lorentz and polarization factor corrections were made according to the method proposed by Arnott.[4] Figure 2 shows the fiber pattern of (+)-poly(BOL).

All calculations were performed on a FACOM M382 computer at Nagoya University Computation Center.

RESULTS AND DISCUSSION

Crystal Data

Only 12 independent diffraction spots were observed in the fiber pattern. Two strong meridional reflections can be confirmed from the X-ray diffraction photographs with fiber axis tilted 11.2° for $l=5$ and 22.8° for $l=10$. All reflections are indexed with a monoclinic unit cell with the following dimensions*; $a=11.79$, $b=14.40$, $c=19.43$Å (fiber period) and $\gamma=98.0°$. The schematic representation of the fiber pattern and the indices of the reflections are presented in Figure 2b. The space group of (+)-poly(BOL) is P2.

The calculated density (D_c) of 1.29 gcm^{-3} is reasonable as compared with the observed one (D_o) of 1.23 gcm^{-3}, if the number of the repeating units (Z) contained in the unit cell is assumed to be 20, taking account of the results of X-ray analysis. The crystal data are given in Table I. The observed and calculated Bragg angles (2θ) and spacings (d) are listed in Table II.

Molecular Structure

In the IR dichroism spectra for the stretching vibrations of both N–H and C=O bonds (Figure 1), the absorptions with the electric vector of the polarized radiation parallel to the fiber axis are remarkably stronger than those with the electric vector perpendicular to the fiber axis. This indicates that both N–H and C=O bonds of (+)-poly(BOL) are roughly

* The monoclinic system is also indicated from the Weissenberg photograph taken with the fiber axis perpendicular to the camera axis.

Table I. Crystal data

Formula unit	$C_6H_9NO_2$
Formula weight	127.14
Space group	P2
Cell constants	
a	11.79 Å
b	14.40 Å
c	19.43 Å
γ	98.0°
Cell volume	3266.6 Å^3
Number of units in the cell (Z)	20
Density obsd (D_o)	1.23 g cm^{-3}
Density calcd (D_c)	1.29 g cm^{-3}

Table II. Observed and calculated spacings and 2θ of the reflections in the fiber pattern

ζ[a]	2θ (obsd)	d (obsd)	2θ (calcd)	d (calcd)	h	k	l
	°	Å	°	Å			
0.16	9.1	9.76	9.1	9.72	$\bar{1}$	1	0
0.33	19.1	4.63	19.1	4.63	$\bar{1}$	3	0
			18.7	4.76	0	3	0
0.47	27.0	3.30	27.1	3.29	1	4	0
			27.4	3.25	$\bar{2}$	4	0
			27.5	3.24	$\bar{3}$	3	0
			27.6	3.23	3	2	0
0.36	21.2	4.18	21.4	4.14	2	2	1
			21.6	4.11	1	3	1
0.13	16.2	5.46	15.6	5.69	1	0	3
0.24	19.5	4.55	19.3	4.61	$\bar{1}$	2	3
0.53	33.9	2.46	34.2	2.62	$\bar{1}$	5	3
			34.3	2.61	0	5	3
			34.1	2.63	2	4	3
			33.6	2.66	4	0	3
0.0	22.9	3.89	22.9	3.89	0	0	5
0.37	30.0	2.98	31.2	2.87	1	3	5
			31.1	2.88	2	2	5
0.58	43.6	2.08	43.6	2.07	1	5	6
			43.9	2.06	$\bar{4}$	3	6
0.22	34.5	2.60	34.4	2.60	0	2	7
0.0	46.8	1.94	46.8	1.94	0	0	10

[a] Multiplied by λ, the wavelength of the X-ray used.

parallel to the fiber axis. The formation of the hydrogen bonds between the N–H and O=C is suggested because of the peak shifts toward the lower wave number sides as compared to the case where the hydrogen bondings do not occur. The hydrogen bonds will roughly be parallel to the fiber axis.

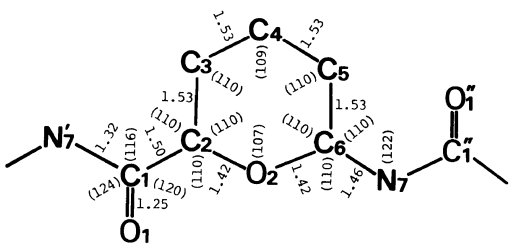

Figure 3. Molecular dimensions adopted for the model construction, together with the numbering of the atoms. Bond angles are in parentheses.

Table III. Definition and values adapted for torsion angles

Angle	Name	Value (°)
C6′–N7′–C1–C2	τ_1	−164.0
N7′–C1–C2–C3	τ_2	Unknown
C1–C2–C3–C4	τ_3	176.0
C2–C3–C4–C5	τ_4	−53.6
C3–C4–C5–C6	τ_5	53.6
C4–C5–C6–N7	τ_6	−176.0
C5–C6–N7–C1′′	τ_7	Unknown

For the model construction, the equations for the helical parameters as a function of torsion angles given by Yokouchi, Tadokoro and Chatani[5] are used. The bond distances and angles used in the model construction are displayed in Figure 3. The definitions of the torsion angles are given in Table III, with the values adopted with reference to the structure of the dimer of (+)-BOL.[6] In (+)-poly(BOL), only two bonds, C1—C2 and C6—N7, are allowed to rotate in a relatively free manner. If the torsion angle around one bond (*e.g.*, τ_7) is assumed to vary, however, the other, τ_2, will be restricted automatically to keep the helical structure. The models having the acceptable fiber period are checked with the cylindrical Patterson map[7,8] as well as the conformational analysis. The isotropic temperature factor of 7.5Å^2 was assigned to all of the atoms. The cylindrical Patterson map synthesized with the observed intensities is shown in Figure 4a.

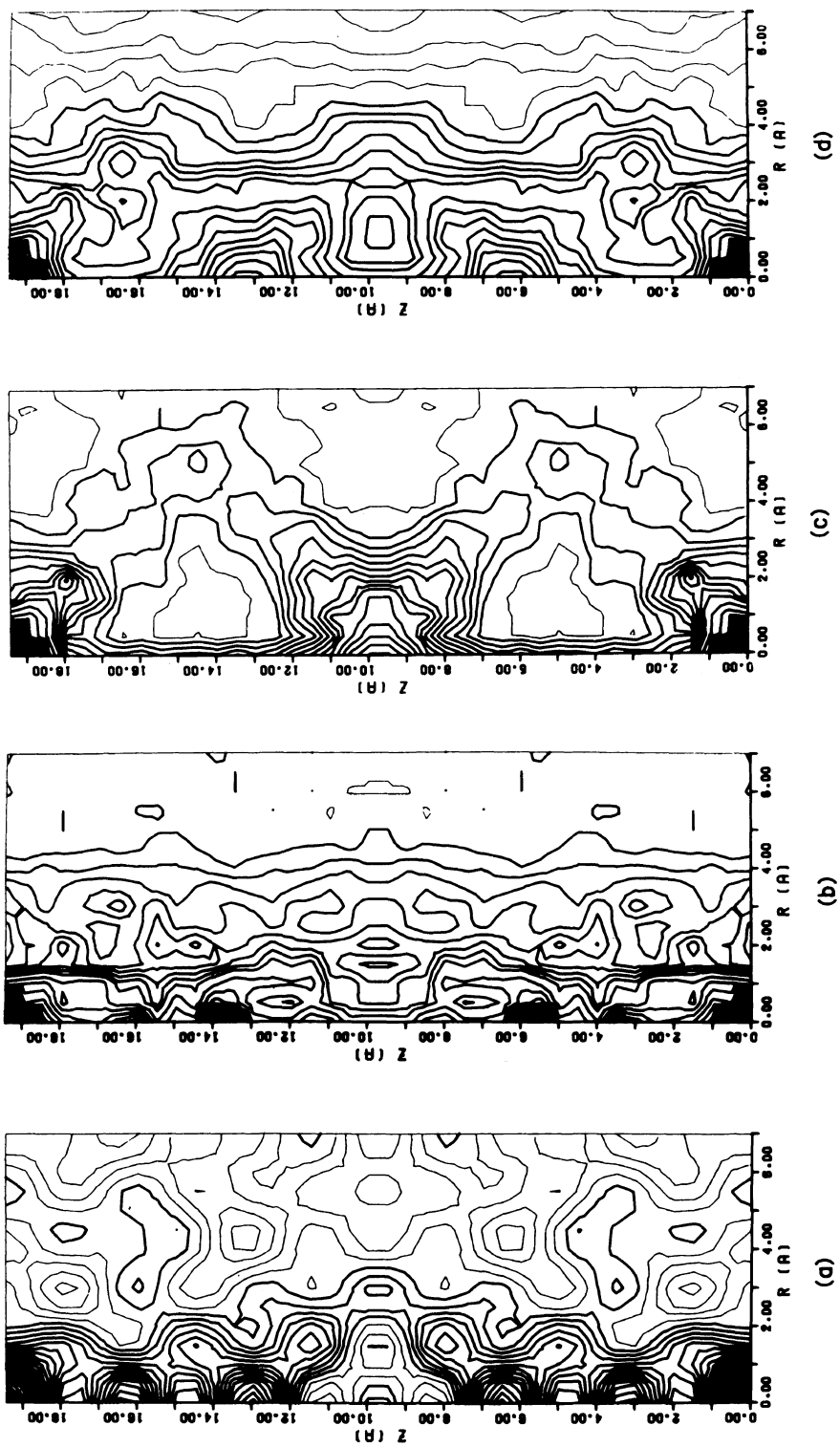

Figure 4. Cylindrical Patterson maps calculated from: a) the observed intensity data; b) 10_3 double-stranded helix model (model II); c) 5_1 double-stranded helix model; d) 10_3 double-stranded helix model (model I).

The X-ray diffraction pattern (Figure 2) indicates that there exists a 5-fold helical symmetry in the structure of (+)-poly(BOL). Therefore the 5_1 and 5_2 helices are first considered. However, both the 5_1 and 5_2 models are not reasonable because of the disagreement between the observed and calculated cylindrical Patterson maps, especially along the *z*-axis, as shown in Figure 4c. For the 5_2 helix, the same discrepancy can be seen along the *z*-axis. As another possible model, a double-stranded 10_3 helix is considered. The double-stranded helices have been proposed to *it*-PMMA[9,10] and poly(ethyleneimine).[11] In the present double-stranded helix two strands are related by the two fold axis which coincides with its helical axis. This results in the fiber period equal to half the identity period of the single helix. For 10_n helices, fibrous sulphur (10_3)[12] and *st*-poly(α-methylvinyl methyl ether) (10_4)[13] were reported besides *it*-PMMA.[9,10] Two plausible models of 10_3 helix, model I and II, are compared in Figure 5. The directions of N–H and C=O bonds are perpendicular to the fiber axis in model I and parallel in model II. Model I, however, is rejected from the IR dichroism spectra and such disagreement between the observed and calculated cylindrical Patterson maps as is obvious from Figure 4a and 4d. In model II the hydrogen bonds (broken lines in Figure 5b) are formed between the two single helices comprising the double-stranded helix. The cylindrical Patterson map synthesized from

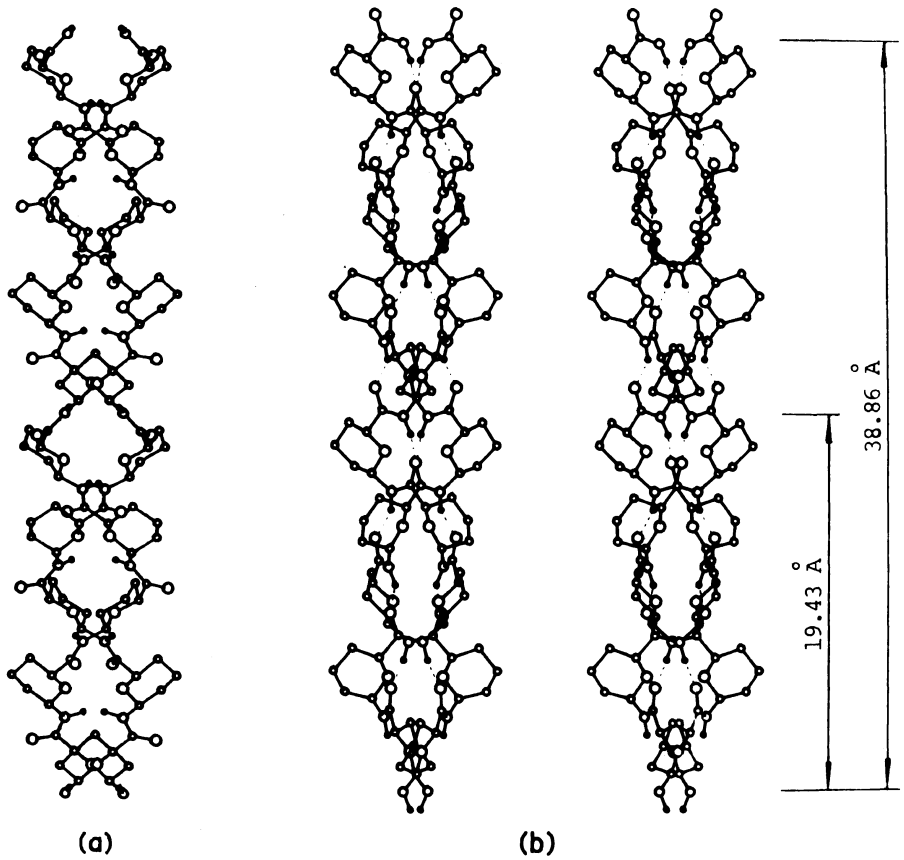

Figure 5. Structures of: a) model I; b) model II (stereo view). The hydrogen bonds are indicated with broken lines.

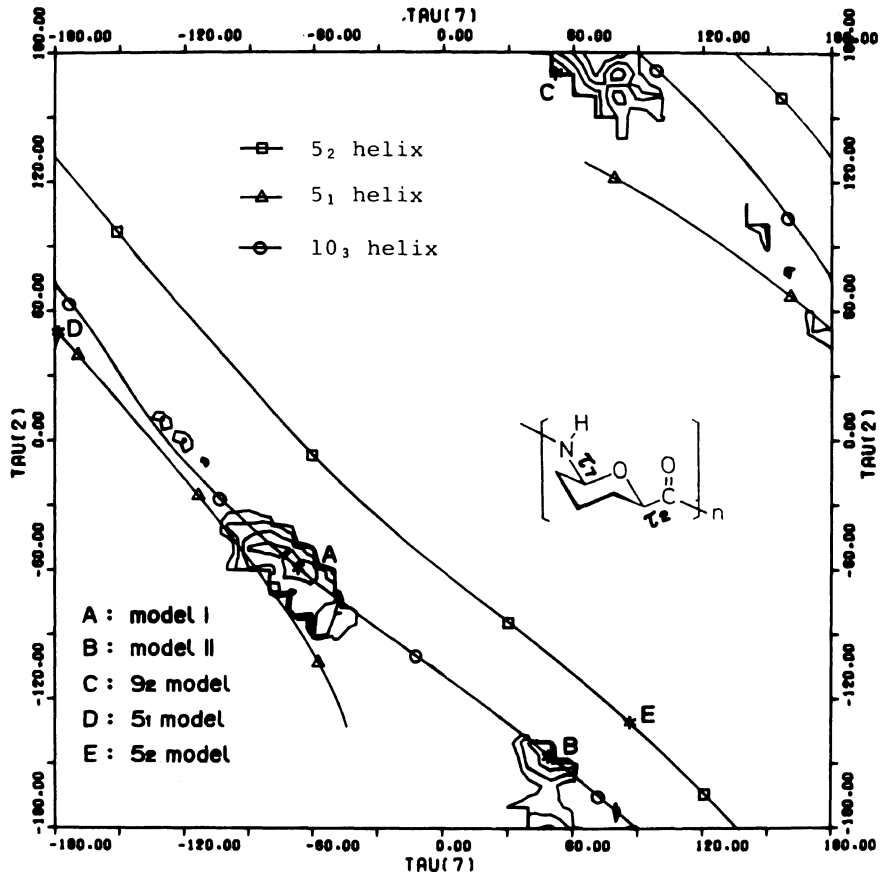

Figure 6. Potential energy map calculated on the basis of double-stranded helix. The relations between τ_2 and τ_7 for both 5_1 and 5_2 helices correspond to τ_1 of 172.0°.

model II is given in Figure 4b. Good agreement between the observed and calculated maps is observed, although along the fiber axis a slight disagreement on z-coordinates of the peaks remains.

The models examined above are all right-handed helices. The left-handed ones have also been tested, but found not to explain the X-ray and IR data.

Conformational Analysis

A potential energy map[14,15] of the double stranded helix based on the two torsion angles, τ_2 and τ_7, is shown in Figure 6. Three energy minima, denominated A, B, and C respectively, are observed. The (τ_2, τ_7) pairs corresponding to the energy minima A, B, and C are (−60°, −65°), (−150°, 50°), and (170°, 50°), respectively. The pair of (τ_2, τ_7) of A was compared with that of model I (−60.0°, −64.6°) and that of B was compared with that of model II (−147.1°, 52.6°). The (τ_2, τ_7) pair of C corresponds to a double-stranded helix with 9_2 symmetry and the identity period of about 23Å. In the 9_2 helix, the orientations of C=O and N–H bonds are in accordance to the results of IR dichroism. This model, however, has difficulties to account for the X-ray data, the helix symmetry and the fiber period.

Thus, model II is supported by the conformational analysis as well as the X-ray data

and IR dichroism information. The double-stranded helix is rather rigid, because of the hydrogen bonds and several close contacts between the two single chains. This may lead to the high thermal transition points and the low solubility of the film of the polymer. Moreover, the double-stranded helix is energetically more stable than the single-stranded one, the difference of potential energy between the two cases being about $9.7/N_0$ kcal per residue (N_0, Avogadro's number). This indicates that the double-stranded helix is energetically rational model for (+)-poly(BOL).

In the crystalline region, there are four polymer chains, that is, two double-stranded helices, passing through the unit cell. The crystal structure of (+)-poly(BOL) will be described elsewhere.

Acknowledgements. The authors are greatly indebted to Prof. T. Kitagawa of Institute for Molecular Science, to Dr. H. Maeda and Prof. S. Ikeda of Department of Chemistry, Nagoya University for the IR measurements, and would also like to thank Toyota Physical and Chemical Research Institute for financial support.

REFERENCES

1. K. Hashimoto and H. Sumitomo, *Macromolecules*, **13**, 786 (1980).
2. H. Sumitomo and K. Hashimoto, *Macromolecules*, **10**, 1327 (1977).
3. H. Sumitomo and K. Hashimoto, "Contemporary Topics in Polymer Science," Vol. 4, W. J. Bailey and T. Tsuruta, Ed., Plenum Press, New York, N. Y., 1984, p 779.
4. S. Arnott, *Polymer*, **6**, 478 (1965).
5. M. Yokouchi, H. Tadokoro, and Y. Chatani, *Macromolecules*, **7**, 769 (1974).
6. T. Yamane, H. Nanayama, T. Ashida, K. Hashimoto, and H. Sumitomo, *Bull. Chem. Soc. Jpn.*, **58**, 2304 (1985).
7. C. H. MacGillavry and E. M. Bruins, *Acta Crystallogr.*, **1**, 156 (1948).
8. R. E. Franklin and R. G. Gosling, *Acta Crystallogr.*, **6**, 678 (1953).
9. H. Kusanagi, H. Tadokoro, and Y. Chatani, *Macromolecules*, **9**, 531 (1976).
10. F. Bosscher, G. ten Brinke, A. Eshuis, and G. Challa, *Macromolecules*, **15**, 1364 (1982).
11. Y. Chatani, T. Kobatake, and H. Tadokoro, *Macromolecules*, **15**, 170 (1982).
12. M. D. Lind and S. Geller, *J. Chem. Phys.*, **51**, 348 (1969).
13. V. Y. Chen, G. Allegra, P. Corradini, and M. Goodman, *Macromolecules*, **3**, 274 (1970).
14. T. Ooi, R. A. Scott, G. Vanderkooi, and H. A. Scheraga, *J. Chem. Phys.*, **46**, 4410 (1967).
15. H. Takahashi, "UNICS-NAGOYA," Nagoya University, Nagoya, Japan, 1981, p 99.